Review

For reprint orders, please contact: reprints@futuremedicine.com

Nanomedicine

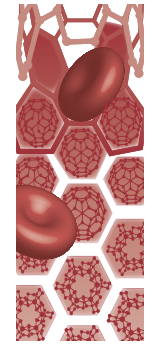

Advances in studies of nanoparticle–biomembrane interactions

Nanoparticles (NPs) are widely applied in nanomedicine and diagnostics based on the interactions between NPs and the basic barrier (biomembrane). Understanding the underlying mechanism of these interactions is important for enhancing their beneficial effects and avoiding potential nanotoxicity. Experimental, mathematical and numerical modeling techniques are involved in this field. This article reviews the state-of-the-art techniques in studies of NP–biomembrane interactions with a focus on each technology's advantages and disadvantages. The aim is to better understand the mechanism of NP–biomembrane interactions and provide significant guidance for various fields, such as nanomedicine and diagnosis.

Keywords: biomembrane • interactions • nanoparticles

Xiao Cong He[‡,1,2], Min Lin[‡,2,3], Fei Li[2,4], Bao Yong Sha[2,5], Feng Xu[3], Zhi Guo Qu[*,1,2] & Lin Wang[*,2,3]

[1]Key Laboratory of Thermo-Fluid Science & Engineering of Ministry of Education, School of Energy & Power Engineering, Xi'an Jiaotong University, Xi'an 710049, PR China

[2]Bioinspired Engineering & Biomechanics Center (BEBC), Xi'an Jiaotong University, Xi'an 710049, PR China

[3]The Key Laboratory of Biomedical Information Engineering of Ministry of Education, School of Life Science & Technology, Xi'an Jiaotong University, Xi'an 710049, PR China

[4]Department of Chemistry, School of Sciences, Xi'an Jiaotong University, Xi'an 710049, PR China

[5]Institute of Basic Medical Science, Xi'an Medical University, Xi'an 710021, PR China

*Authors for correspondence:
Qu ZG: zgqu@mail.xjtu.edu.cn;
Wang L: wanglin0527@126.com

The advances in nanomaterials and nanotechnology in the past few years have resulted in the development of various nanoparticles (NPs) and their widespread applications in cosmetics [1], textiles [2], building materials [3], nanodevices [4], nanomedicine and diagnostics [5]. NPs enter an organism through various approaches (e.g., the respiratory system [6], skin absorption [7], intravenous injection and implantation [8]) and subsequently induce a series of complicated reactions. For beneficial applications, NPs can be rapidly internalized by cells, which has been applied for cancer gene therapy [9,10], bioimaging and phototherapy [11,12]. By contrast, NPs may change the cell membrane thickness and integrity [13] and induce pore formation in the membrane [14] and oxidative stress [15], resulting in nanotoxicity. During all of these processes, NPs need to interact with biomembranes (e.g., the cell membrane), which are basic barriers for access to cells. Therefore, understanding the underlying mechanism of the NP–biomembrane interactions is important for enhancing the beneficial effects of NPs and avoiding potential nanotoxicity.

Various approaches have been developed in order to study NP–biomembrane interactions, including experimental observations [16–18], theoretical analysis [19] and numerical simulations [20–23]. These approaches are complementary in this field. For instance, molecular dynamic simulations can detail the whole dynamic process of NP–lipid bilayer interactions at the molecular level, but they are limited within the temporal (near-nanosecond) and spatial (near-nanometer) scale. Experimental studies can investigate more complicated and larger systems (NP–cell systems); however, they can only obtain end-point results and cannot reach the high resolution of molecular dynamic simulations. Furthermore, many modeling studies still need to be validated by experimental results. Therefore, combining experimental studies with mathematical and numerical modeling studies will provide more deep insight into the NP–biomembrane interactions.

In order to better understand the NP–biomembrane interactions, this article reviews the state-of-the-art techniques involved in the study of NP–biomembrane interactions. In the experimental studies, NP–biomembrane interactions can be assessed by recording the characteristic changes of the NP–biomembrane system, such as the morphological,

Future Medicine part of fsg

thermal, electromagnetic, optical and electrochemical properties and response of cells. The property changes during NP–biomembrane interactions and the corresponding characterization techniques are reviewed in the following sections, with a focus on their advantages and disadvantages. Furthermore, the mathematical and numerical modeling studies of NP–biomembrane interactions are also reviewed. Finally, a future perspective of this field is presented.

Methods based on morphology change

Generally, four mechanisms are involved in NP–biomembrane interactions, including adsorption onto the membrane surface, pore formation, direct penetration and endocytosis (Figure 1). With different NP properties, the mechanisms of NP–biomembrane interactions are different. For instance, 20-nm diameter polystyrene NPs can adsorb onto the lipid bilayer [24]. Cationic NPs can induce pore formation in the biomembrane, such as gold NPs (AuNPs) and SiO_2 NPs with cationic side chains [25,26] and poly(amidoamine) dendrimers [27]. Small NPs (e.g., metal clusters [28]), needle-shaped NPs (e.g., single-carbon nanotubes [29]) and NPs bounded with cell-penetrating peptides can directly penetrate the membrane [30]. Various NPs can be endocytosed by cells, such as carbon nanotubes [31,32], AuNPs [33], polymer NPs [34,35] and silica NPs [36,37]. The effects of NP surface properties on NP–biomembrane interactions has been reviewed in detail previously [38]. Furthermore, another article on the nano–bio effect has comprehensively reviewed NP properties, their cellular uptake and potential toxicity [39].

No matter which mechanism the NP–biomembrane interactions belong to, the interactions can induce morphological changes in the system, such as NP location, thickness and pore formation of the membrane, as well as membrane bending. These morphological changes can reflect the process of NP–biomembrane interactions [40]. Therefore, characterization of the morphological changes is the most intuitive and effective method for studying the effects of NPs on biomembranes. At present, four main microscope technologies, including transmission electron microscopy (TEM), scanning electron microscopy (SEM), atomic force microscopy (AFM) and scanning ion conductance microscopy (SICM), have been used to observe these morphological changes.

TEM- & SEM-based techniques

With the advantages of high spatial resolutions (several nanometers for SEM and fractions of nanometers for TEM), TEM and SEM are commonly used to observe morphological changes of NP–biomembrane systems. Based on the location of NPs and the cell shape, the NPs adsorbed onto the cell surface, passing through the membrane and trapped in endosomes can be observed via SEM and TEM (Figure 2). By SEM testing, small MCM-41-type mesoporous silica NPs and iron oxides are observed to adsorb onto the surface of red blood cells (RBCs) (Figure 2A) [40] and human lymphoblasts [41], respectively. SEM images show that 1D nanomaterials, such as multiwalled carbon nanotubes and gold nanowires, enter cells in a vertical approach (Figure 2B) [20]. As for the 2D nanometerials, TEM

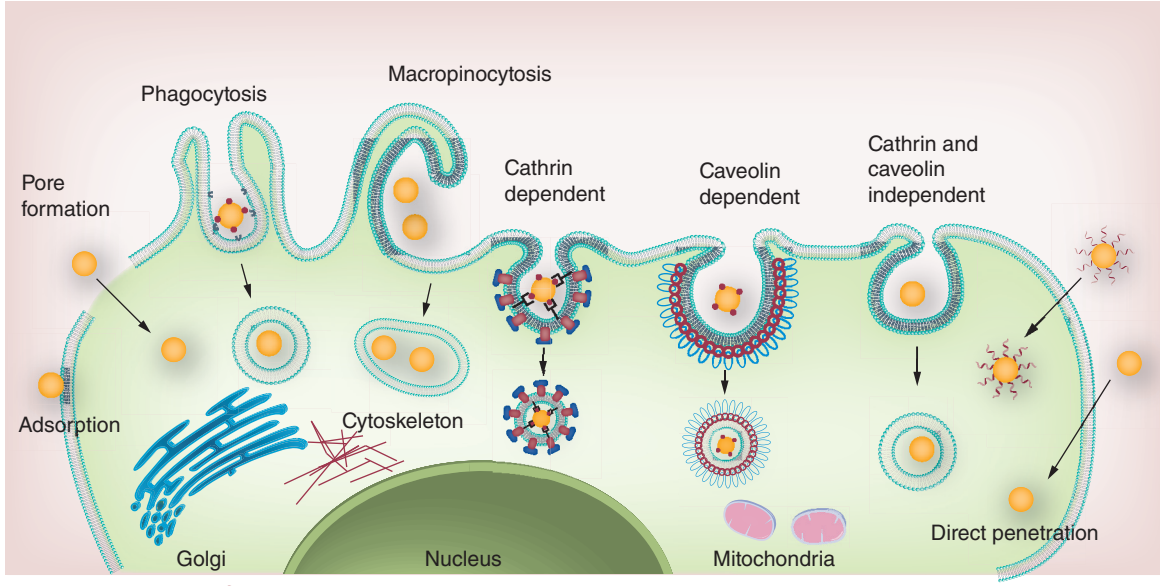

Figure 1. Schematic of the nanoparticle–biomembrane interaction mechanism. Four mechanisms, including adsorption onto the membrane surface, pore formation, direct penetration and endocytosis, are involved in nanoparticle–biomembrane interactions.

images indicate that 2D few-layer graphene microsheets show edge or corner penetration [42]. PEG-modified magnetic NPs [43] and iron oxide NPs [41] trapped in lysosomes and endosomes separately after endocytosis are observed by SEM. In addition to the aforementioned static processes, a semidynamic process of the cellular uptake of SBA-15-type mesoporous silica NPs is observed by TEM, which shows that SBA-15-type mesoporous silica NPs are gradually engulfed by RBCs (Figure 2C) [40]. TEM and SEM are well suited to observing morphological changes of NP–cell interactions. Although researchers have obtained images of different cellular uptake processes, the images were from parallel experiments at different NP–biomembrane interaction stages [40]. Given the fixation step before imaging and the vacuum environment required during imaging for most TEM and SEM instruments, researchers can only obtain static information from samples. Thus, a real-time monitoring technique with high resolution is needed in order to improve experimental studies in this field.

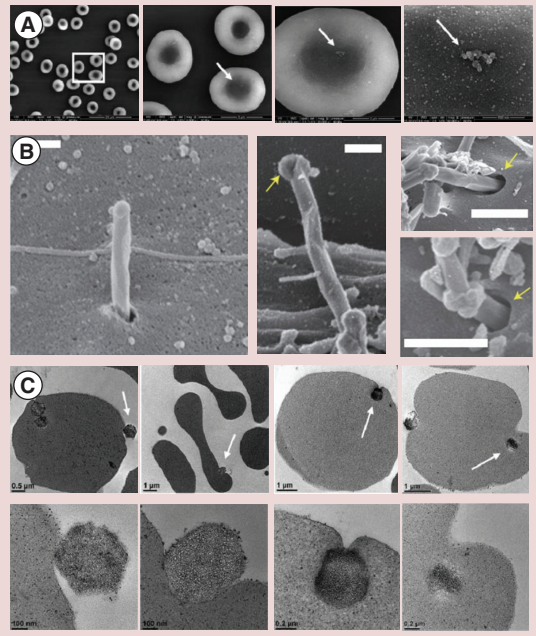

Figure 2. Scanning electron microscopy and transmission electron microscopy images of nanoparticle–cell interactions. (A) Scanning electron microscopy images showing that small MCM-41-type mesoporous silica nanoparticles adsorb onto the surface of red blood cells. From left to right: images increase in magnification with features highlighted with white squares or arrows [40]. **(B)** Scanning electron microscopy images showing that multiwalled carbon nanotubes enter into murine liver cells via a vertical approach (scale bar: 300 nm). Left: multiwalled carbon nanotubes undergoing high-angle tip entry; middle: arrow shows carbon shell; right: arrows show membrane invaginations at the point of entry [20]. **(C)** Transmission electron microscopy images showing the cellular uptake process of SBA-15-type mesoporous silica nanoparticles interacting with red blood cells. The images at the bottom are magnifications of the corresponding upper images [40].
(A & C) Reproduced with permission from [40]; **(B)** reproduced with permission from [20].

AFM-based techniques

AFM can map local physical properties of samples by sweeping a probe across the sample surface to dynamically record the morphologies and properties of biological samples based on the interaction between the probe tip and the sample surface. Several NP–biomembrane interactions, including pore formation, adsorption onto a membrane and envelopment by a membrane, can be observed by AFM [44–47]. For instance, pore formation on the supported lipid bilayer (SLB) induced by small-sized silica NPs (1.2–22 nm) (Figure 3) [48] and amine-terminated dendrimers (G7) are observed by AFM [49,50]. Through comparing the topographical data with corresponding phase contrast of AFM images, the peptide (MSI-78) is found to selectively absorb onto the Lα (liquid–crystalline fluid phase) regions of the lipid bilayer [51]. For silica NPs with larger sizes of approximately 22 nm, the AFM images show that NPs with a smooth surface can be completely enveloped by a lipid bilayer, whereas NPs with a bumpy surface can only be partially enveloped [52]. AFM is particularly suitable for observing biological samples due to two advantages: one is its application in aqueous solutions under physiological conditions and the other is its ability to obtain surface morphological details with a resolution of fractions of a nanometer [53]. However, AFM has disadvantages of a limited scanning area (maximum ~150 × 150 μm) and a slow scanning rate. Furthermore, the possible damage to biomembrane surfaces during scanning with a hard tip limits its application in imaging soft and mobile cells. Therefore, it is commonly used to observe the morphology changes of NP–SLB systems. SLBs with a planar bilayer structure supported by a solid substrate (e.g., mica or silicon) are stable enough to withstand AFM scanning (Figure 4B) [44,48,52]. In addition, with a defined composition, SLBs can isolate the effects of individual factors (e.g., lipid, protein and cholesterol) on the interaction processes (Table 1).

SICM-based techniques

Rather than applying a physical force to the sample as in AFM, SICM uses a cone-shaped glass pipette with a nanometer diameter (i.e., a nanopipette) filled with electrolytic solution as the probe. By scanning sample surfaces with a constant distance and monitoring the

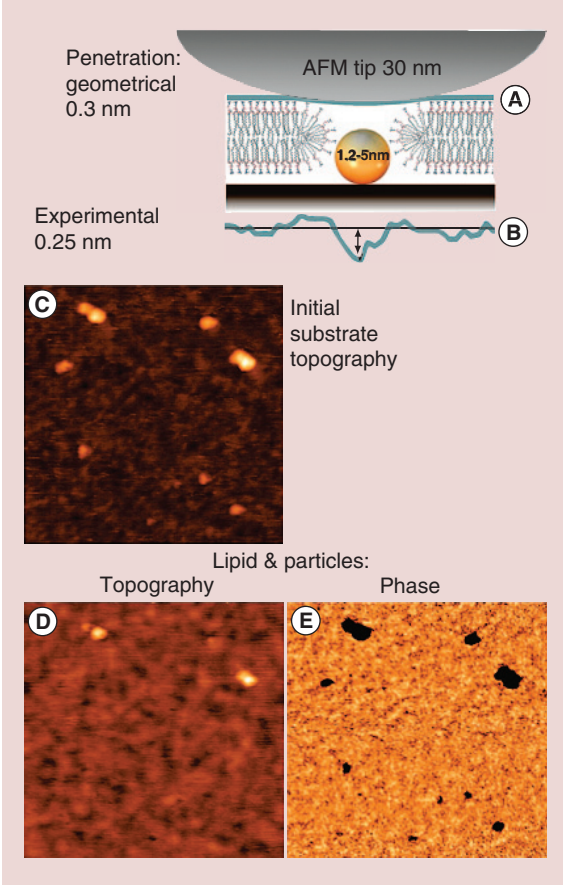

Figure 3. Atomic force microscopy images of interactions between silica nanoparticles with sizes of 1.2–5 nm and lipid bilayers. (A) Schematic and **(B)** AFM curves of pore formation induced by nanoparticles. **(C)** Topography image of the substrate with nanoparticles. **(D)** Topography and **(E)** phase images of the substrate with 1–8 nm nanoparticles and lipid deposited on it [48].
AFM: Atomic force microscopy.

ionic current between the tip opening and the sample surface, SICM can investigate morphological changes of samples in real time, especially soft materials, in aqueous solution and with a high resolution, without direct interactions of the probe tip and sample surface [54,55]. For example, membrane damage induced by NPs are recorded by SICM [56–59]. Results show that the membranes are damaged and holes form when human alveolar epithelial type 1-like cells are exposed to amine-modified polystyrene latex NPs [56]. By combining SICM with the patch-clamp technique, the morphological changes of human alveolar epithelial A549 cells interacting with ZnO NPs are tracked, where membrane damage is observed after 100 μg/ml of ZnO NP treatment (Figure 5) [57]. In addition, by combining SICM and confocal microscopy, the adsorption of fluorescent Cy3-labeled single virus-like NPs on COS-7 cell surfaces can be recorded [58]. Although SICM has strengths in imaging soft biomembrane surfaces at a nanometer-scale resolution, its complex operation process and slow scan rate limit its wide application in this field (Table 2).

Methods based on thermal properties

The lipid structure is temperature dependent, and each kind of lipid has a characteristic temperature at which it undergoes a transition between the gel and liquid phase. This phenomenon makes it possible to characterize the details of interactions by characterizing the thermal properties of the NP–biomembrane system, as long as the NPs will also undergo enthalpy changes with temperature changes. Differential scanning calorimetry (DSC) is a thermoanalytical technique. Through simultaneous heating or cooling of the sample and reference materials in order to maintain equal temperature conditions, the DSC technique measures the relationship of temperature and heat flow differences between the sample and the reference materials. The NP–biomembrane interactions can be reflected by the phase changes, which can be derived from the calorimetric curves.

Various NPs penetrating into the lipid bilayer have been observed by DSC through calorimetric curves [60–62]. For instance, the interaction of idebenone (IDE)-loaded solid lipid NPs (SLNs) with multilamellar vesicles (MLVs) is investigated using the DSC method (Figure 6) [60]. The calorimetric curves show that for the curves of IDE-loaded SLNs, the peak at 46°C disappears in the subsequent scans with elapsed time. For the curves of MLVs, the main peak moves to a low temperature and broadens. These results indicate that the IDE-loaded SLNs move inside the MLVs and IDE is released. For other phase-change NPs, such as G3/G4 dendrimers [61] and peptides [62], details regarding insertion into the model membrane are also observed by DSC. The results indicate that dendrimers can interact with both the head and tail groups of lipids. Regarding the interactions of an amphipathic peptide RL16 and dimyristoylphosphatidylglycerol (DMPG) MLVs, these have little effect on the main peak of the calorimetric curves, which indicates that RL16 cannot penetrate deeply into the lipid core [63]. As for the case of cationic linear peptide analogs (LPAs), the results show that LPA-C_4 and LPA-C_7 are restrained at the interface between the lipid and water, while LPA-C_{11} can penetrate into the lipid bilayer [62].

The DSC method has advantages in terms of characterizing the physical and chemical changes of samples (e.g., the insertion process, bond rupture and binding) via a user-friendly operation. NP–biomembrane interactions characterized by DSC are based on

the enthalpy changes of the system; therefore, the NPs are limited to phase-change materials, such as lipids, dendrimers and peptides. Because the system suffers at elevated temperatures, this method is not suitable for cells. DSC is generally used to characterize mixed systems of NPs and lipid vesicles. The structure of a lipid vesicle [64] is shown in Figure 4C. Furthermore, the recording of calorimetric curves is generally a time-consuming process (taking several hours).

Methods based on electromagnetic properties

Nuclear magnetic resonance (NMR), x-ray reflectivity (XR) and neutron reflectivity (NR) are carried out in order to characterize structural changes during NP–biomembrane interactions based on the changes of the electromagnetic properties of the system.

If the number of protons or neutrons in a nucleus is odd, the nucleus has an intrinsic nonzero spin. These nuclei can absorb and re-emit electromagnetic radiation with specific resonance frequencies when in an external magnetic field. This signal can be characterized by NMR and reflect molecular structure details. Therefore, NMR has been applied to capturing the dynamics and structural details of NP–biomembrane systems through characterization of the system's isotopes, such as ^{13}C, ^{15}N, ^{13}P, ^{2}H and protons [65]. For instance, ^{31}P- and ^{2}H-NMR are used to characterize the interactions between fullerenol and the lipid head and tail groups, respectively [66]. The ^{31}P-NMR results show the effects of fullerenol on the motion and average orientation of the head groups, while the ^{2}H-NMR results show that fullerenol brings minimum perturbation to the tail groups. These results indicate that fullerenol

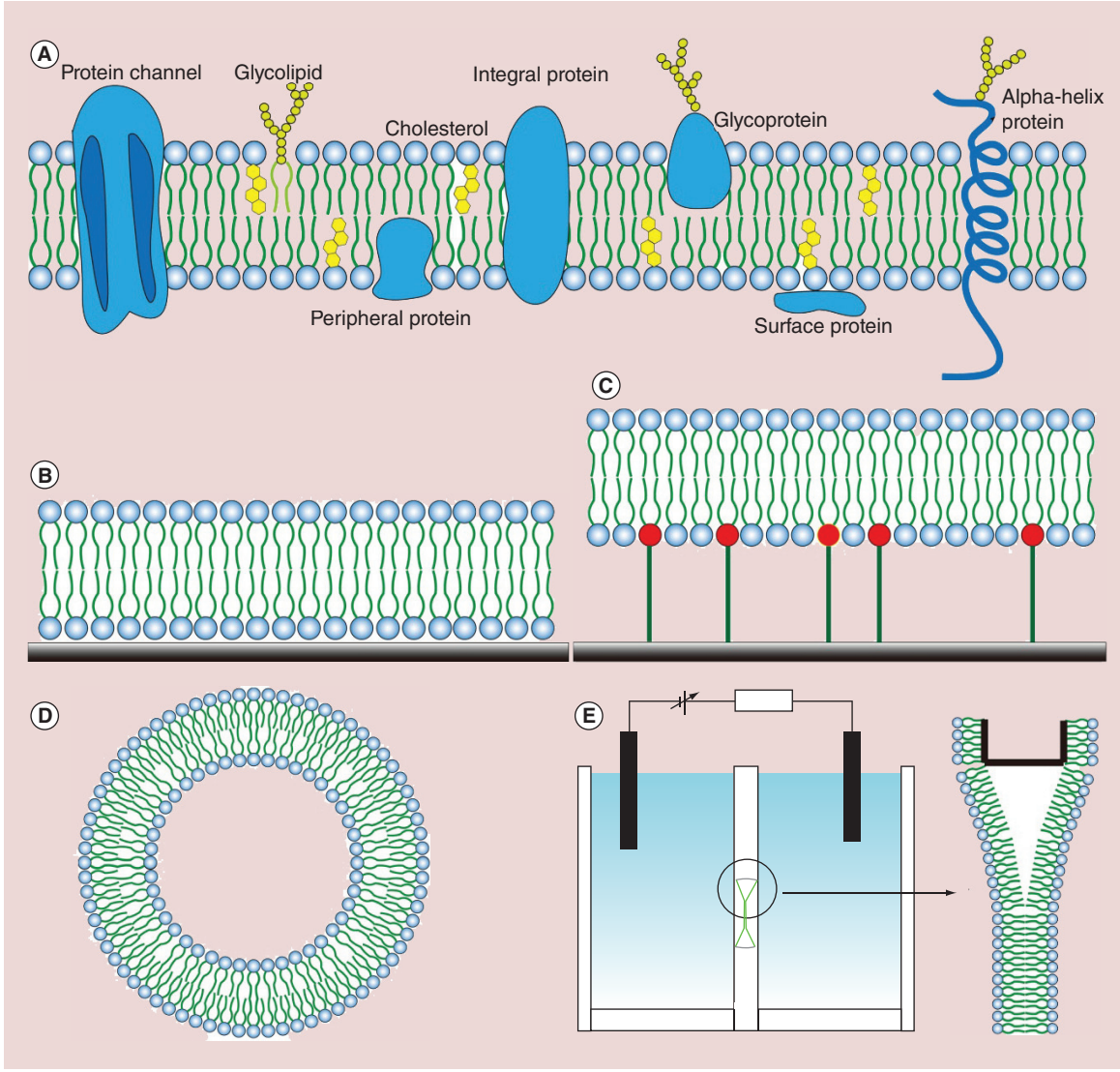

Figure 4. Various model lipid bilayers used in experimental studies. **(A)** Cell membrane; **(B)** supported lipid bilayer; **(C)** tethered lipid bilayer; **(D)** lipid vesicles; and **(E)** black lipid bilayer.

Table 1. Comparison of different biomembranes.

Biomembrane	Stability	Surface sensitivity	Preparation convenience	Composition	Structure	Characteristics
Cell membranes	Yes	Yes	No	Lipids, proteins and others	Complicated composition	Cell response reflecting interactions
Supported lipid bilayers	Yes	Yes	No	Lipids	Planar bilayer structure supported by a solid substrate (e.g., mica or silicon)	Stable enough to suffer from hard instruments (e.g. AFM)
Tethered lipid bilayers	Yes	Yes	No	Lipids; proteins	Uses chemical anchors (e.g., polymer, protein and peptide) to tether the lipids to the solid substrate	Two sides are free to the solvents
Vesicles	No	No	Yes	Lipids; proteins	Spherical lipid bilayer shell	Sizes range from tens of nanometers to hundreds micrometers
Black lipid membranes	No	No	Yes	Lipids	Suspended planar lipid bilayer	Used to investigate membrane electrophysiological properties, but limited by a short lifespan

AFM: Atomic force microscopy.

remains at the water–bilayer interface. In addition to the aforementioned 1D NMR spectra, the molecular structures are more detailed in 2D NMR spectra, such as nuclear Overhauser effect spectroscopy. The proton signal in the ^{1}H–^{1}H nuclear Overhauser effect NMR spectra indicates that a dendrimer inserted into a lipid bilayer interacts with the lipid acyl chains [67]. It should be noted that the inserted dendrimer (G5) can induce more restriction to the lipid tails than G7 [68]. NMR techniques are able to provide detailed information of NP–model biomembrane interactions at the molecular level, but the system must use isotopes, such as ^{13}C, ^{15}N, ^{13}P, ^{2}H and protons. Furthermore, the disturbance of the solvents should also be considered. If the solvents are abundant in protons, the NP–biomembrane system or the solvents need to be perdeuterated.

XR and NR technologies are tools used to investigate thin films and interfaces at a submicron scale. Reflectivity depends on the surface complexity when a beam of light (x-ray or neutron) is shot at the interface. The surface morphology details can be obtained by recording the reflectivity curves. XR is used to monitor morphological changes during the interactions between the supported dipalmitoylphosphatidylcholine (DPPC) lipid bilayer and the transcription-activating facto-derived peptides (TDPs) [69]. The XR reflectivity curves indicate that the TDPs adsorb onto the outer membrane surface with increasing time, and then transfer to the inner side of the lipid bilayer. However, because of the insensitivity of XR to in-plane structures, the pore formation of the membrane cannot be observed. Taking account of the high penetrating and typical nonperturbing properties of neutrons, NR is used to characterize the creation of defects in the TDP–membrane translocation [69]. Furthermore, NR measurements observe that cubosome particles and the lipid bilayer have strong interactions and exchange lipids at the interface [70,71]. By combining this with ellipsometry, the results show that increasing the solution can induce the release of the adsorbed NPs [71].

Methods based on optical properties

Various light microscopies and spectroscopy technologies have been used to characterize NP–biomembrane interactions based on the optical properties of the system. In many cases, the most powerful forms of light microscopy are based on fluorescence [72]. In this section, we summarize the technologies based on fluorescence, such as confocal laser scanning microscopy (CLSM), and some spectroscopy technologies, including ultraviolet and visible spectroscopy, surface-enhanced Raman spectroscopy and Fourier transform infrared spectroscopy (FTIR).

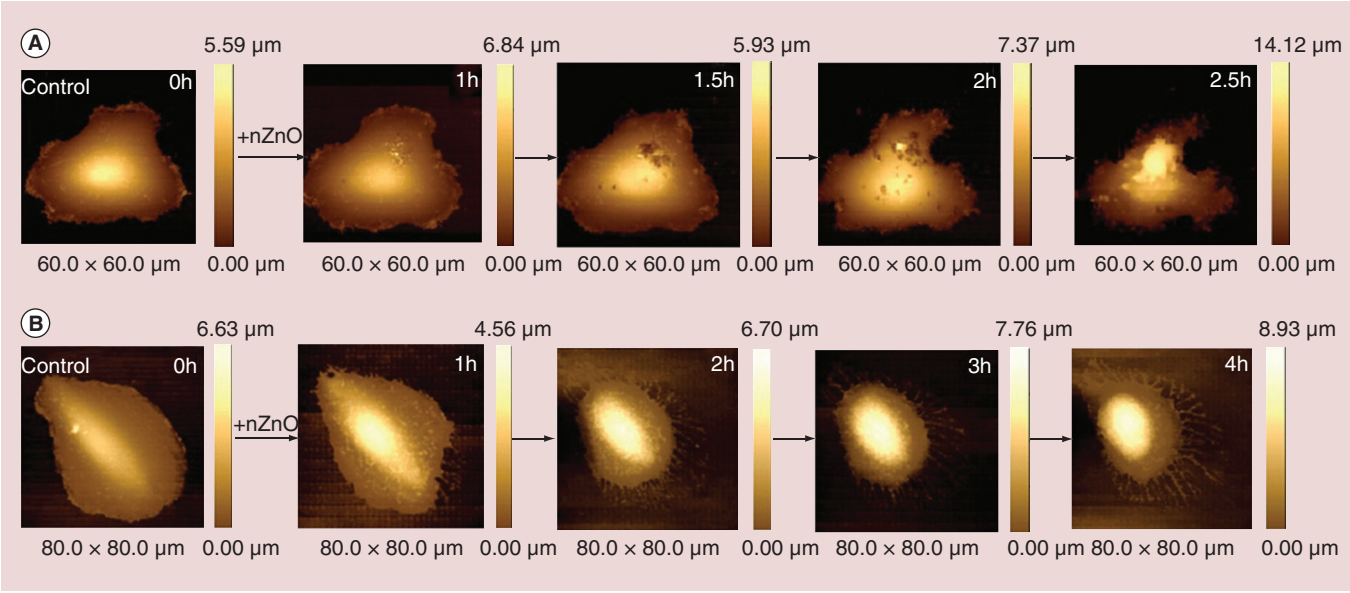

Figure 5. Continuous scanning ion conductance microscopy images of A549 cell monolayers exposure to ZnO nanoparticles.
Acute damage to cells induced by the nanoparticles is observed within 1.5 h [57].
nZnO: Zinc oxide nanoparticle..

Technologies based on fluorescence

Some classes of NPs, such as quantum dots (QDs) and rare earth NPs, are intrinsically fluorescent materials, whereas other NPs can be generally derivative with fluorescent markers such as fluorescein-5-isothiocyanate (FITC). In addition, the biomembane can be stained by various fluorescent dyes including lipophilic carbocyanine dyes. By recording the fluorescence of these NPs and biomembranes in the NP–biomembrane system, the system's behavior can be revealed.

CLSM has attracted significant attention because of its capacity to obtain high-resolution optical images at different depths. The addition of a laser light source, scanning system and conjugate focusing system on the optical microscope allows CLSM to enlarge its functions, including obtaining high-resolution 3D images, hierarchical scans, semiquantitative analyses of fluorescence intensity and simultaneous characterizations of multiple fluorescent labels. For large-sized cells and giant unilaminar vesicles (GUVs), which are tens of micrometers in size, interactions between NPs and cells or GUVs are investigated by CLSM. Through CLSM image analysis, NP–biomembrane interactions, such as internalization by various cells, adsorption onto the membrane surface and the induction of membrane damage, can be observed. For instance, CLSM images show the cellular uptake of lipid–QDs bilayer vesicles by human epithelial lung cells (A549) [73] and amine-modified PEGylated QDs by alveolar epithelial cells [74]. Through recording the FITC fluorescence by CLSM, AuNPs transporting membrane-impermeable FITC-labeled protein into a variety of cell lines can be observed [75]. In addition, 20-nm polystyrene NPs with cationic surfaces adhering strongly to the lipid bilayer of GUVs [24] are shown in CLSM images. Through the characterization of the leakage of fluorescent dextran, which is coated by GUVs, the membrane damage induced by polystyrene NPs can be observed [24]. Furthermore, semiquantified and quantified data, including the NP fluorescence intensity on the membrane surface [24], the internalization rate of QDs [76] and the amount of nanowire penetration into living cells [77], can also be obtained. However, compared with TEM and SEM, CLSM is limited by its reduced sensitivity and spatial resolution. In addition, the markers labeled on NPs and biomembrane may affect the interactions.

Single-particle tracking technology is able to observe the motion of single particles and obtain the trajectories of particles through fluorescent or optical labels. Parameters including the diffusion coefficient and mean square displacement can be obtained by random trajectory analysis. In order to investigate the NP–biomembrane interactions, NP trajectories are traced by tracking their fluorescence, such as with single-walled carbon nanotubes [78], fluorescently labeled peptides [79,80] and QDs [81]. With single-particle tracking technology, the trajectories of cellular uptake and expulsion of single-walled carbon nanotubes (length: 130–660 nm) are obtained through intrinsic photoluminescence [78]. The quantified data, such as the lateral mobility of the peptide on the GUV surface, are also obtained

Table 2. Comparison of various technologies for the experimental study of nanoparticle–biomembrane interactions.

Techniques	NP	Biomembrane	Interactions	Advantages	Disadvantages	Ref.
Methods based on system morphology						
TEM, SEM	Silica	RBCs	Engulfment	High spatial resolution (several nanometers for SEM and fractions of a nanometer for TEM) and simple operation	Static detection; sample fixation	[40]
	MWCNT	Mouse AML12 liver cells; human mesothelial cells	Endocytosis			[20]
	Iron oxide NPs	Human lymphoblasts	Adsorption; endocytosis			[41]
	Magnetic NPs	Human fibroblasts	Endocytosis			[43]
AFM	Silica NPs	DMPC SLBs	Pore formation; envelopment	Scanning in a liquid environment; fractions of a nanometer resolution; dynamic detection	Limited image range; slow scan rate; hard tip	[48,52]
	PAMAM dendrimers	SLBs	Pore formation			[49,50]
SICM	Polystyrene latex NPs	Human alveolar epithelial type 1-like cells; cardiomyocyte	Pore formation	Dynamic recording of living biological samples under physiological conditions; nanometer spatial resolution; noninvasive characterization	Limited image range; slow scan rate	[56]
	ZnO NPs	Human alveolar cells; epithelial A549 cells	Membrane damage			[57]
	Fluorescent Cy3-labeled single virus-like particles	Monkey COS-7 cells	Adsorption			[58]
Methods based on thermal properties						
DSC	Solid lipid NPs	Multilamellar vesicles	Penetration	Simple operation; provides information on the penetration process and bond rupture and binding	Limited to phase change materials; large time cycles	[60]
	Dendrimers	DMPC/DPPC liposomes	Penetration			[61]
	Cationic linear peptides	DPPC/DPPS liposomes	Penetration			[62]

AFM: Atomic force microscopy; AgNP: Silver nanoparticle; AuNP: Gold nanoparticle; CLSM: Confocal laser scanning microscopy; DMPC: Dimyristoylphosphatidylcholine; DOPC: Dioleoylphosphatidylcholine; DPPC: Dipalmitoylphosphatidylcholine; DPPS: Dipalmitoylphosphatidylserine; DSC: Differential scanning calorimetry; FTIR: Fourier transform infrared spectroscopy; GUV: Giant unilaminar vesicle; ICP-MS: Inductively coupled plasma mass spectrometry; ICP-OES: Inductively coupled plasma optical emission spectroscopy; MDA: Malondialdehyde; MWCNT: Multiwalled carbon nanotube; NMR: Nuclear magnetic resonance; NP: Nanoparticle; NR: Neutron reflectivity; PAMAM: Poly(amidoamine); QCM-D: Quartz crystal microbalance with dissipation monitoring; QD: Quantum dot; RBC: Red blood cell; ROS: Reactive oxygen species; SEM: Scanning electron miscroscopy; SECM: Scanning electrochemical microscopy; SERS: Surface-enhanced Raman spectroscopy; SICM: Scanning ion conductance microscopy; SLB: Supported lipid bilayer; SWNT: Single-walled carbon nanotube; TEM: Transmission electron microscopy; UV-vis: Ultraviolet and visible spectroscopy; XR: X-ray reflectivity.

Table 2. Comparison of various technologies for the experimental study of nanoparticle–biomembrane interactions (cont.).

Techniques	NP	Biomembrane	Interactions	Advantages	Disadvantages	Ref.
Methods based on electromagnetic properties						
NMR	Dendrimers	Lipid bilayers	Penetration	Provides structural information on the molecule; dynamic detection	NPs need to contain isotopes and protons	[67]
	Fullerenol	DPPC/cholesterol lipid bilayers	Adsorption			[66]
XR, NR	Peptides	DPPC SLBs	Penetration	Provides information on thin films and interfaces	High cost, low measurement resolution	[69]
	C_{60}	Multilamellar vesicles	Pore formation			[129]
Methods based on optical properties						
CLSM	QDs	Rat tumor cells	Penetration	Obtains 3D images with high resolution; hierarchical scan; semiquantitative analysis of fluorescence intensity; simultaneous detection of multiple fluorescent labels	High cost; needs fluorescent labels; reduced sensitivity and spatial resolution compared with TEM and SEM	[76]
	Lipid–QD bilayer vesicles	Human epithelial lung cells (A549)	Internalization			[73]
	Amine-modified PEGylated QDs	Alveolar epithelial cells	Penetration			[74]
	AuNPs	HeLa cells	Endocytosis			[75]
	Dendrimers	HEK293T and HeLa cell	Pore formation			[130]
	Silica	DOPC GUVs	Membrane wrapping			[131]
	Polystyrene	DOPC GUVs	Adsorption			[24]
Single-particle tracking	SWNTs	NIH3T3 fibroblast cells	Endocytosis	Obtains the trajectories of particles; diffusion coefficient and mean square displacement	Needs fluorescent or optical labels	[78]
	Peptides	GUVs	Penetration			[79,80]
UV-vis	AuNPs	Human breast cancer cells	Cellular uptake concentration	Simple operation; provides structural information of molecules	Not able to provide information on dynamic processes	[17,132]
SERS	Ibuprofen	Lipid bilayers	Penetration			[84]
FTIR	Hydroxyapatite NPs	RBCs	Adsorption			[83]

AFM: Atomic force microscopy; AgNP: Silver nanoparticle; AuNP: Gold nanoparticle; CLSM: Confocal laser scanning microscopy; DMPC: Dimyristoylphosphatidylcholine; DOPC: Dioleoylphosphatidylcholine; DPPC: Dipalmitoylphosphatidylcholine; DPPS: Dipalmitoylphosphatidylserine; DSC: Differential scanning calorimetry; FTIR: Fourier transform infrared spectroscopy; GUV: Giant unilaminar vesicle; ICP-MS: Inductively coupled plasma mass spectrometry; ICP-OES: Inductively coupled plasma optical emission spectroscopy; MDA: Malondialdehyde; MWCNT: Multiwalled carbon nanotube; NMR: Nuclear magnetic resonance; NP: Nanoparticle; NR: Neutron reflectivity; PAMAM: Poly(amidoamine); QCM-D: Quartz crystal microbalance with dissipation monitoring; QD: Quantum dot; RBC: Red blood cell; ROS: Reactive oxygen species; SEM: Scanning electron miscroscopy; SECM: Scanning electrochemical microscopy; SERS: Surface-enhanced Raman spectroscopy; SICM: Scanning ion conductance microscopy; SLB: Supported lipid bilayer; SWNT: Single-walled carbon nanotube; TEM: Transmission electron microscopy; UV-vis: Ultraviolet and visible spectroscopy; XR: X-ray reflectivity.

Table 2. Comparison of various technologies for the experimental study of nanoparticle–biomembrane interactions (cont.).

Techniques	NP	Biomembrane	Interactions	Advantages	Disadvantages	Ref.
Methods based on electrochemical properties						
SECM	AgNPs	HeLa cells; fibroblast cells	Adsorption; penetration	Scan under physiological conditions; real time; *in situ*; label-free; noncontact; obtains chemical properties of cells	Micrometer spatial resolution; slow scan rate	[86,87]
	ZnO NPs	Human nasopharyngeal epithelial cancer cells	Respiration rate			[88]
Methods based on responses of cells						
ROS and MDA assay	CdSe/ZnS core–shell QDs	Chinese hamster lung cells	ROS	Provides information about cell responses to NPs and cytotoxicity of NPs	Gives limited information about NP–biomembrane interactions	[133]
	Amorphous silica	Mouse keratinocytes	ROS			[107]
	ZnO NPs	Zebrafish embryos	MDA			[100]
	CuO NPs	Podocytes	MDA			[101]
Cell viability assays	TiO_2	Fish cells	Cell viability	Simple operation; provides cell viability information and cytotoxicity of NPs	Gives limited information about NP–biomembrane interactions	[104]
	SWNTs	Breast cancer cells	Cell viability			[1]
Hemolysis assay	NPs	RBCs	Pore formation	Simple operation; provides pore formation information	Limited to RBCs and pore formation detection	[92]
	Copolymers	RBCs	Pore formation			[111]
	Lipid-based liquid crystalline materials	RBCs	Pore formation			[134]
Other techniques						
QCM-D	Polymers	SLBs	Adsorption	Studies molecular adsorption/desorption and binding kinetics; real time; surface sensitive	Limited to surface adsorption detection	[123]
	Dendrimers	SLBs	Adsorption			[124,135]
ICP-MS, ICP-OES	AuNPs	Human fibroblast cells (1BR3G)	Penetration	Detects low concentrations with high precision and sensitivity	Limited to metals and several non-metals	[125]
	AuNPs; fullerenes	SLBs	Adsorption			[126,127]
Electrical methods	AuNPs	Black lipid bilayers	Adsorption	Obtains quantified parameters of membrane adsorption	Black lipid bilayers limited by a short lifespan	[128]

AFM: Atomic force microscopy; AgNP: Silver nanoparticle; AuNP: Gold nanoparticle; CLSM: Confocal laser scanning microscopy; DMPC: Dimyristoylphosphatidylcholine; DOPC: Dioleoylphosphatidylcholine; DPPC: Dipalmitoylphosphatidylcholine; DPPS: Dipalmitoylphosphatidylserine; DSC: Differential scanning calorimetry; FTIR: Fourier transform infrared spectroscopy; GUV: Giant unilaminar vesicle; ICP-MS: Inductively coupled plasma mass spectrometry; ICP-OES: Inductively coupled plasma optical emission spectroscopy; MDA: Malondialdehyde; MWCNT: Multiwalled carbon nanotube; NMR: Nuclear magnetic resonance; NP: Nanoparticle; NR: Neutron reflectivity; PAMAM: Poly(amidoamine); QCM-D: Quartz crystal microbalance with dissipation monitoring; QD: Quantum dot; RBC: Red blood cell; ROS: Reactive oxygen species; SEM: Scanning electron miscroscopy; SECM: Scanning electrochemical microscopy; SERS: Surface-enhanced Raman spectroscopy; SICM: Scanning ion conductance microscopy; SLB: Supported lipid bilayer; SWNT: Single-walled carbon nanotube; TEM: Transmission electron microscopy; UV-vis: Ultraviolet and visible spectroscopy; XR: X-ray reflectivity.

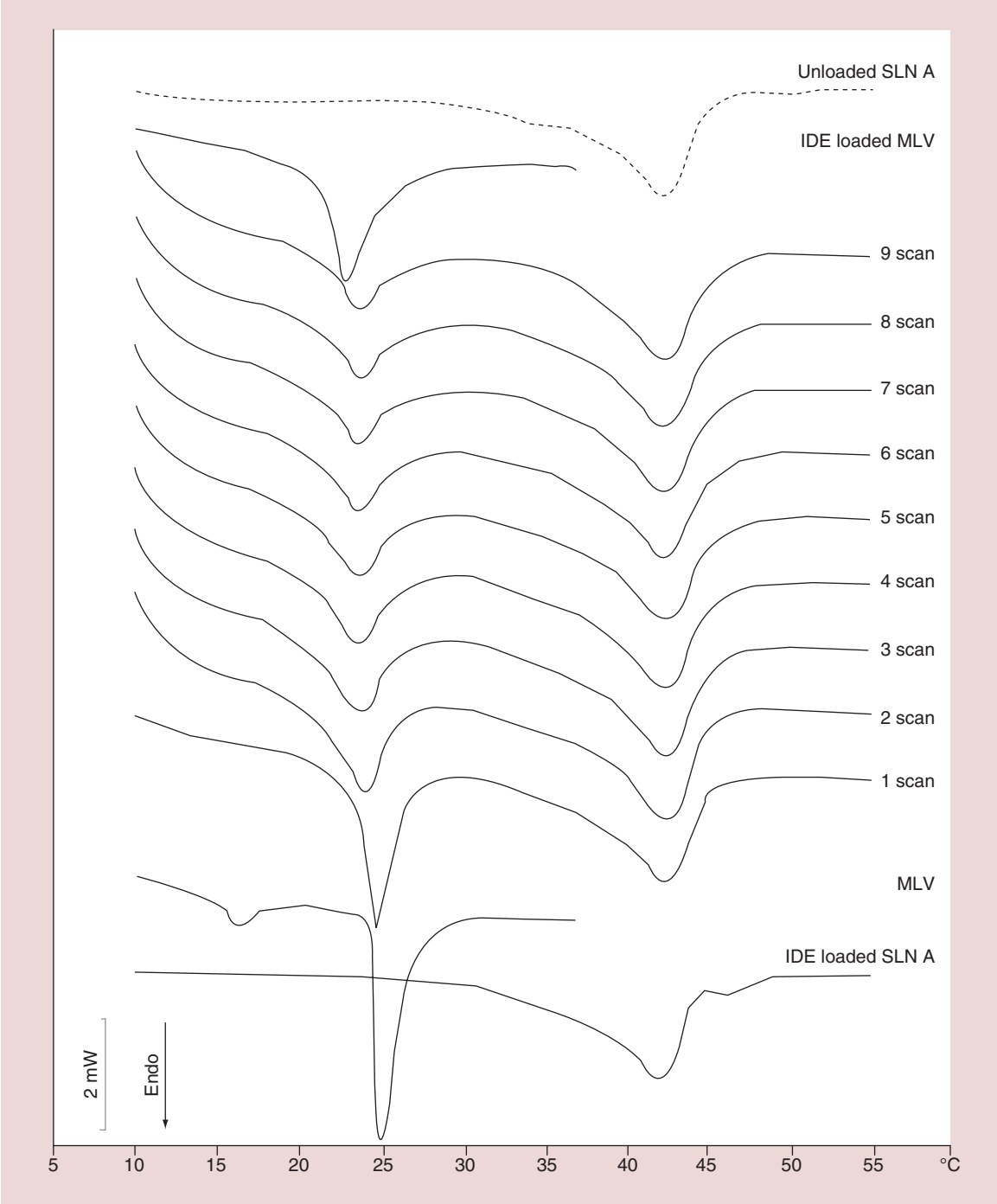

Figure 6. Differential scanning calorimetric curves of idebenone-loaded solid lipid nanoparticles interacting with multilamellar vesicles [60].
Endo: Endothermic; IDE: Idebenone; MLV: Multilamellar vesicle; SLN A: Solid lipid nanoparticle containing isoceteth-20/glyceryl oleate.

[80]. In order to investigate the early stages of the NP (peptide HIV1-Tat-modified NP) binding and cellular uptake, effort has been made to combine single-particle tracking technology with CLSM [82]. This newly developed technology is able to capture the landing process of NPs before cellular uptake in a 3D manner in real time (Figure 7). This method provides a powerful tool for investigating the dynamics of the landing process before cellular uptake.

Spectroscopy technologies

A specific type of molecule can absorb radiation with

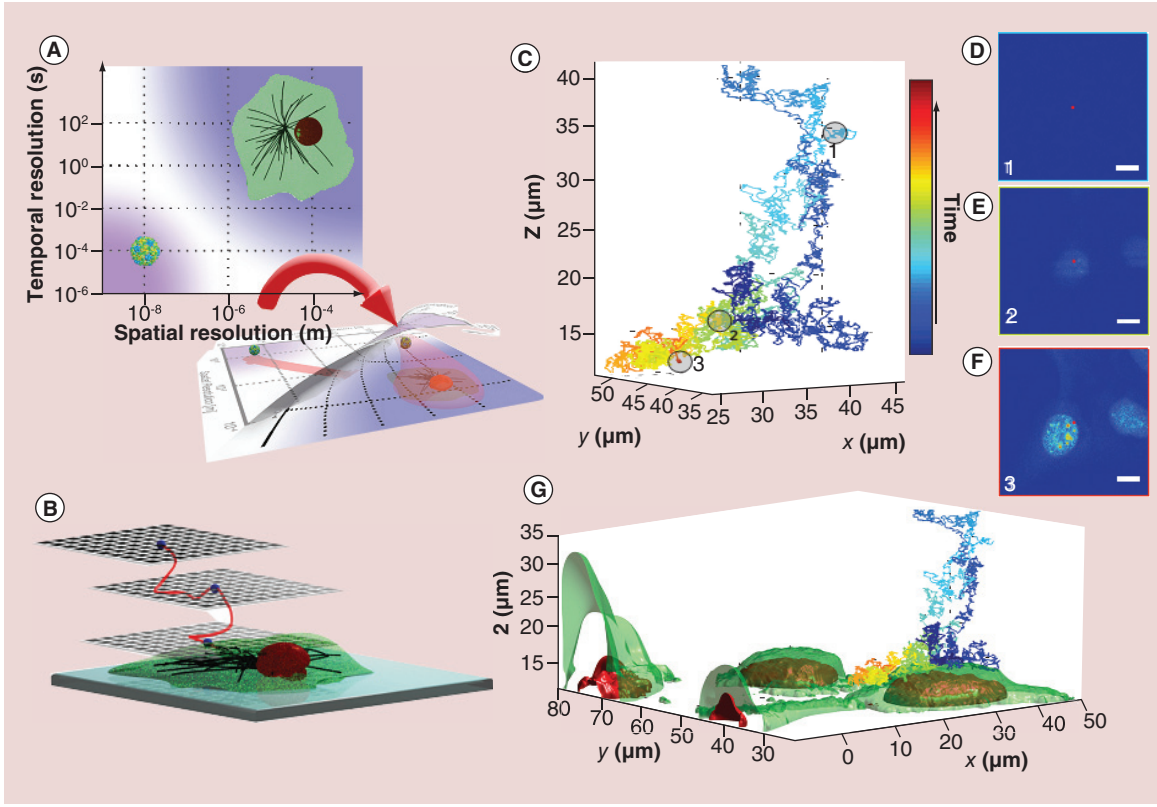

Figure 7. 3D images of the early stages of cellular uptake in real time. (A) Schematic of the method for measuring delivery vehicles and live cells simultaneously. **(B)** Through combining with the single-particle detection technology, 3D images of the nanoparticle landing on a live cell can be obtained. **(C)** 3D trajectory of the nanoparticle. **(D–F)** The confocal images (scale bars: 10μm) correspond to points 1–3 in **(C)**, respectively. **(G)** 3D reconstruction of the data [82].

a characteristic wavelength. Therefore, the structural information of samples can be obtained by recording the characteristics of the absorbed radiation (transmittance and absorbance) from the samples. Spectroscopy technologies provide molecular bond information simply and sensitively in NP–biomembrane interaction studies. For instance, FTIR was used to analyze the interaction mechanism between RBCs and hydroxyapatite (HAP) NPs [83]. The adsorption of sialic acid on the surface of HAP NPs is observed by comparing the FTIR spectra of HAP NPs before and after adsorption. Semiquantified information can be obtained, such as the increased ratio of ibuprofen penetrating into the bilayers for different ibuprofen concentrations monitored by normalized surface-enhanced Raman spectroscopy intensity [84] and the cellular uptake number of AuNPs as monitored by ultraviolet and visible spectroscopy, through the extinction spectra and calibration curves [17]. Although the spectroscopy technologies can provide detailed structural information of these interactions, they are not able to provide insight into the dynamic processes of the interactions and generally need to be combined with intuitive imaging technologies, such as TEM and SEM.

Methods based on electrochemical properties

Scanning electrochemical microscopy (SECM) is another type of scanning probe microscopy technique that uses a microelectrode as the tip to scan over a specimen surface in an electrolyte solution [85]. In addition to the applications performed using AFM and SICM, SECM can obtain the chemical information of the sample of interest. Therefore, SECM was applied to investigate NP–biomembrane systems based on their electrochemical property changes. For example, through recording the oxygen reduction current of cells, the cellular activity can be obtained. Therefore, SECM offers a nondestructive characterization of chemical changes of cells under NP attack. For example, SECM demonstrates that the number of silver NPs adsorbed onto HeLa cell surface and the morphological changes of these cells can be observed simultaneously [86]. Moreover, by recording the consumption of dissolved O_2, the viability of living fibroblast cells under silver NP attack can be characterized by SECM [87]. In addition, ZnO NP attack on nasopharyngeal cancer cells can also be characterized by SECM [88]. This result shows that the cell respiration rate is affected by the ZnO

NP dose and decreases with time. SECM is well suited for studying NP–cell interactions not only due to its ability to scan morphological changes (as with AFM and SICM), but also due to it being able to observe the chemical changes (e.g., cell oxygen consumption and respiration rate) of cells under NP attack. These chemical changes can reflect the living status of cells. Therefore, the SECM approach is widely used to assess the cytotoxicity of NPs. However, SECM has a limited resolution, which is normally in at a micro-scale level.

Methods based on the responses of cells

Various live cells are used in NP–biomembrane interaction experiments [89,90], such as cancer cells (e.g., HeLa cells [91]), RBCs [92] and epithelial cells (e.g., human alveolar epithelial type 1-like cells; Figure 4A [56]). Compared with NP–model lipid membrane interactions, the use of live cells offers several advantages, including that the NP–cell membrane system can be easily observed using optical microscopes because cells are generally several micrometers in scale [89,93]. Moreover, the direct investigation of NP–biomembrane interactions can be realized through cell responses [40,90], such as the changes of reactive oxygen species (ROS), malondialdehyde (MDA), cell viability and the hemolysis of RBCs, among other responses. However, the plasma membrane composition and cell microenvironment are very complicated, making it challenging to isolate the effects of individual factors on the NP–biomembrane interactions.

The characterization of ROS is widely used in NP–cell interaction studies [94]. The accumulation of ROS can perturb the balance of oxidants and antioxidants in biological systems [95,96], which can steal electrons from the cellular lipid membrane, resulting in lipid peroxidation and cell damage [97]. MDA is a stable end product of lipid peroxidation resulting from ROS through the degradation of polyunsaturated lipids [98]. Abnormal level of MDA can alter the structural integrity of the cell membrane, which acts as a marker for cell membrane injury [99]. Increased MDA levels are found in zebrafish embryos, podocytes and lung fibroblasts after exposure to ZnO, CuO and AuNPs [100–102].

Cell viability assays, including the neutral red assay, trypan blue assay, LIVE/DEAD® test (Life Technologies, Shanghai, China) and lactate dehydrogenase (LDH) assay, are applied to observe the adverse effects of NPs [103], but these methods are indirect. The exposure of NPs causes damage to the membrane and cell death [1,104]. Following this, the dyes, such as neutral red, trypan blue and an ethidium homodimer, can permeate and mark the damaged plasma membranes or dead cells [1,104]. In addition, NPs can damage the membrane integrity and lead to the release of intracellular components (e.g., LDH). In addition, the concentration of released LDH is proportional to the number of damaged or lysed cells [105–107]. However, the cell viability assays can only test the cell growth situation without giving detailed information on the NP–biomembrane interactions. Therefore, the cell viability assays are generally combined with morphology observation techniques, such as TEM, SEM, plasma mass spectroscopy and CLSM, in order to quantify the

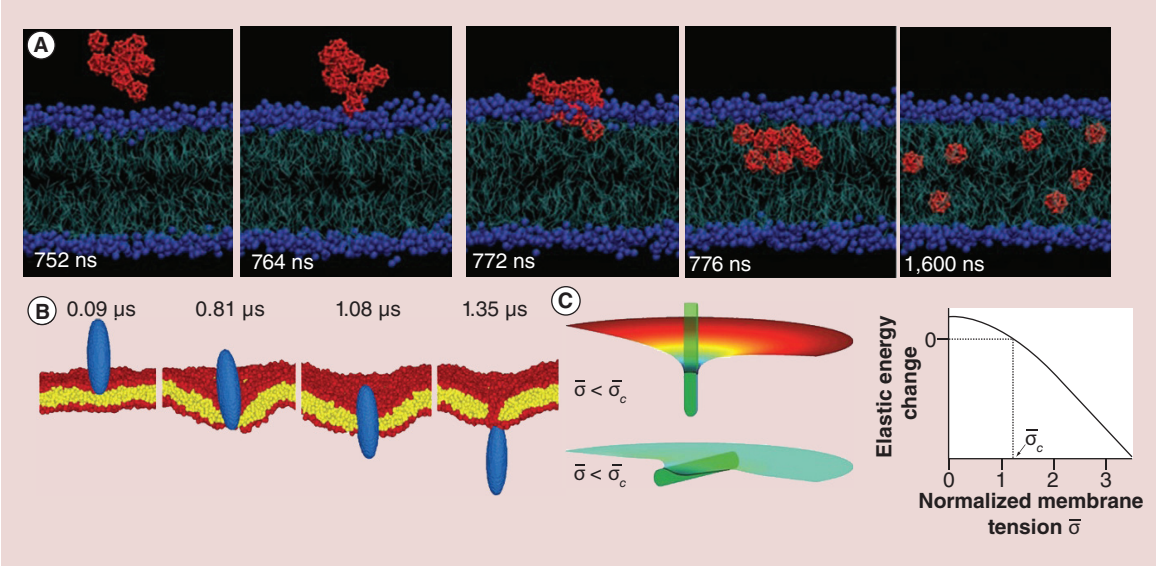

Figure 8. Mathematical and numerical modeling of nanoparticle–biomembrane interactions. **(A)** Snapshots of a cluster of ten fullerenes penetrating into the dioleoylphosphatidylcholine (DOPC) lipid bilayer [117]. **(B)** The translocation of ellipsoids with vertical starting orientations [21]. **(C)** Perpendicular entry modes and parallel surface adhering modes with different membrane tensions [120].

number of NPs in cells [55] and to determine the cellular uptake [108].

Many NPs, such as cationic NPs [109] and silver NPs [110], can induce pore formation in the membrane. Researchers have performed hemolysis assays in order to verify membrane damage during interactions between NPs and RBCs [92,111]. For instance, positively charged polyelectrolyte-coated NPs can induce hemolysis. However, this is not the case for negatively charged polyelectrolyte-coated NPs because of the repulsion between the negatively charged membrane and NPs [92]. The hemolysis assay can only verify membrane rupture. Therefore, for other interactions, such as direct penetration and endocytosis, its combination with other appropriate technologies is required.

Mathematic & numerical modeling

Due to the small sizes of the NPs and biomembrane (<100 nm), the quick response timescale (near-microsecond) of the process and the soft nature of the biomembrane, it is a challenge for experimental studies to determine detailed NP–biomembrane interaction pro-

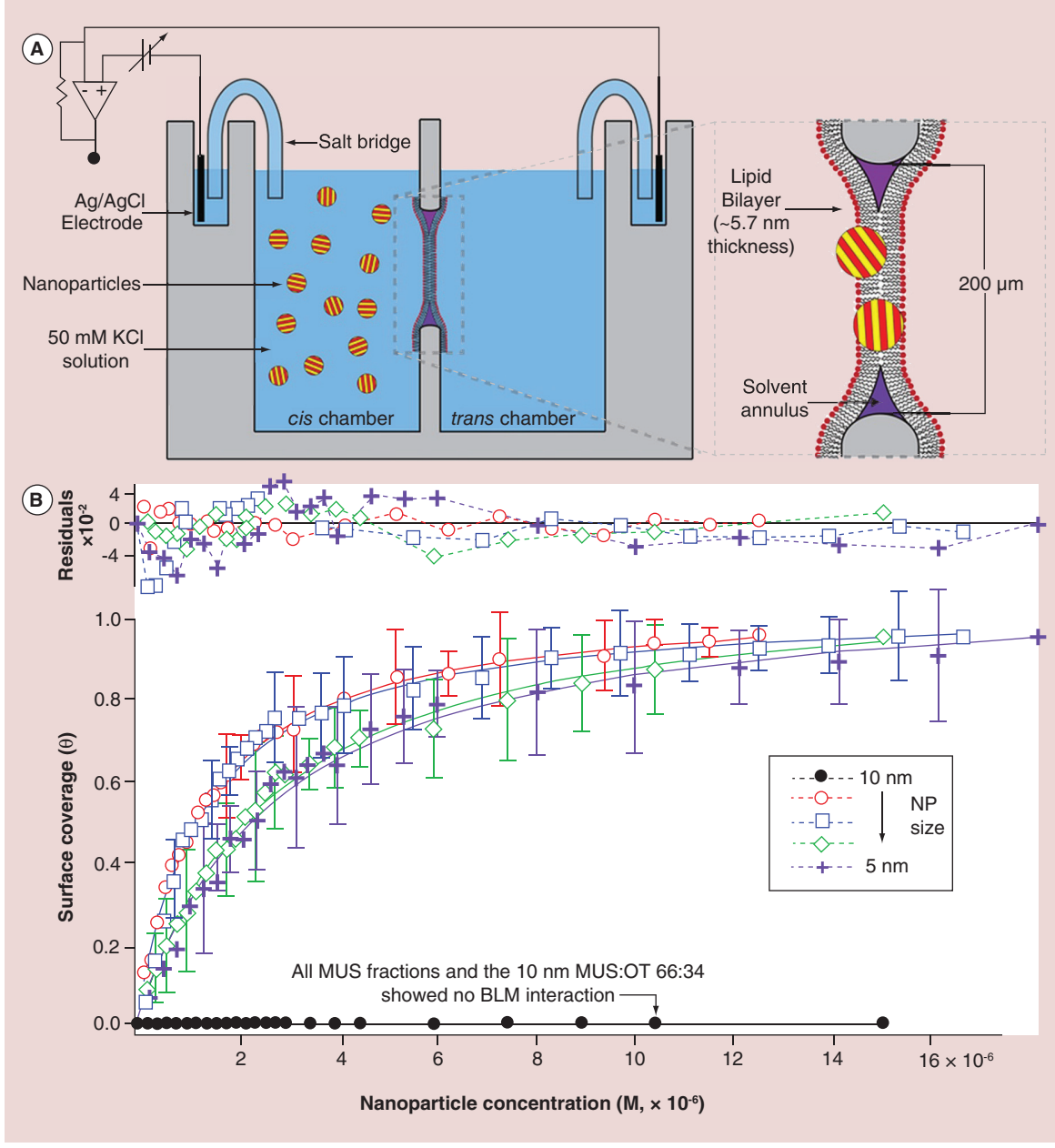

Figure 9. The electrical method for quantifying striped mixed monolayer-coated gold nanoparticles interacting with a black lipid membrane. (A) Schematic of experimental system. **(B)** The relationship between surface coverage and NP concentration for each size of NP [128].
BLM: Bilayer lipid membrane; MUS: 11-Mercaptoundecane sulfonate; NP: Nanoparticle; OT: Octanethiol.

cesses in real time and with a high resolution. As complementary methods, molecular dynamic simulation and mathematic modeling can provide deep insights into the interactions at the nanoscale. In particular, molecular dynamic simulation provides detailed information of the whole interaction process with a temporal (near-femtosecond) and spatial (near-Ångstrom) resolution that is not yet accessible to the existing experimental techniques. In this section, molecular dynamic simulation and mathematic modeling methods used in this field are reviewed.

Molecular dynamic simulation, which is based on the classical Newtonian laws of motion, can describe the trajectories of molecules and determine the dynamic processes of NP–biomembrane interactions. There are two types of dynamic models: atomistic models and coarse-grained models [112]. The simulation unit adopted in each model is different. Atomistic models employ a single atom as the simulation unit; thus, they can determine detailed atom–atom interactions. For instance, when interacting with the membrane, the small molecules benzocaine [113] and C_{60} clusters [114] prefer to spread homogeneously near the membrane center, and the preferred position for C_{60} is approximately 6–7 Å away from the bilayer center [115]. However, all-atom molecular dynamic simulations are limited by their small temporal (near-nanosecond) and spatial (near-nanometer) scale. Coarse-grained models combine a cluster of atoms, molecules or chemical groups as a 'bead' offering a longer time (millisecond) and larger length (micrometer) scale [116]. For instance, the whole process of ten fullerenes penetrating into a lipid bilayer can be simulated by coarse-grained molecular dynamic simulation (Figure 8A) [117]. However, when simulated by all-atom molecular dynamics, this interaction is divided into two segments: the fullerenes are initially inside or outside of the membran because of the small temporal scale of all-atom molecular dynamics [114]. Dissipative particle dynamic simulation is another coarse-grained model that has been used to study the translocation processes of NPs with different shapes (e.g., spheres and ellipsoids particles; Figure 8B) [21]. Results show that the NP shape and initial orientation have significant effects on interactions. For instance, the penetration time is shorter for NPs with a vertical initial orientation than a horizontal initial mode.

Despite molecular dynamic simulations, other mathematical models have also been developed in order to investigate NP–biomembrane interaction mechanisms [118–120]. For instance, a mathematical model has been built to study the mechanism of ligand–receptor-based endocytosis. Results show that NP size plays an important role in the interactions and there is an optimal size for the shortest wrapping time [119]. As for the endocytosis of 1D nanomaterials, a modeling study found that NPs perpendicularly penetrate the membrane with small tension, while they interact in parallel with membranes at large tension (Figure 8C) [120]. Another study investigated the effect of particle elasticity on cellular uptake. The results indicate that the membrane fully wraps stiffer NPs more easily than softer particles [19].

Other techniques

In addition to the techniques mentioned above, other techniques, such as quartz crystal microbalance with dissipation monitoring (QCM-D), inductively coupled plasma (ICP) and electrical methods are applied to the study of biomembrane responses under NP attack.

Based on interfacial acoustic sensing, the QCM-D technique determines the adsorption/desorption and binding kinetics of molecules in real time, without labeling and in a surface-sensitive fashion [121,122]. During QCM-D measurements, the adsorption of NPs can change the dissipation factor, and the mass uptake or release at the sensor surface can change the resonance frequency. For example, human insulin-loaded polycationic polymer NPs interacting with SLBs can be studied using QCM-D [123]. Results show that cationic NPs collapse after adsorbing onto the negatively charged membrane, whereas adsorption is not observed on the positively charged membrane. Combined with QCM-D and fluorescence microscopy, the dendrimer that changes the membrane property has been found. Results show that the dendrimer induces increasing membrane stiffness after binding onto the membrane, even at a low concentration. The increased stiffness causes membrane instability and collapse of the vesicles [124].

ICP mass spectrometry (ICP-MS) and ICP optical emission spectroscopy (ICP-OES) technologies are used in the study of NP–biomembrane interactions. After ionizing the samples by ICP, ICP-MS separates and quantifies ions through a mass spectrometer in order to measure the ion concentration. The concentration of the cellular uptake of AuNPs functionalized with peptidic biomolecules is determined by ICP-MS. The results show that the internalized NP concentration increases for the cationic bioconjugates [125]. As for ICP-OES, ICP is used to excite atoms and ions to emit electromagnetic radiation with characteristic wavelengths. Based on the intensity of this radiation, the concentration of the elements in the sample can be determined by ICP-OES. The mass of AuNPs and fullerenes accumulated in the aqueous phase or lipid phase can also be measured by ICP-OES in order to study their distributions within water or the lipid

bilayer [126,127]. ICP-MS and ICP-OES are good at characterizing low concentrations of materials with high precision and sensitivity. However, the characterized materials are limited to metals and some nonmetals (e.g., carbon and phosphorus).

Recently, an electric method was used to quantify striped mixed monolayer-coated AuNPs interacting with a black lipid membrane (Figure 9) [128]. Alhough this involved the monitoring of the capacitive increase of the black lipid membrane in the process of NP adsorption and was based on the Langmuir model, quantified parameters of membrane adsorption, such as surface coverage, the adsorption equilibrium constant and free energy change, were obtained. This provides a method for investigating NPs adsorbed onto black lipid membranes both qualitatively and quantitatively. Alhough black lipid membranes (Figure 4E) are well suited to investigating the electrophysiological properties of the membrane, this model membrane is restrained by its short lifespan (hours).

Conclusion & future perspective

The fast-growing field of nanotechnologies and nanomaterials requires a fundamental understanding of NP–biomembrane interactions. Significant achievements in the understanding of the underlying interaction mechanisms have been made by characterizing the morphological, thermal, electromagnetic, optical and electrochemical properties of NP–biomembrane systems, the responses of cells and the development of mathematical and numerical modeling. Different interactions, including adsorption, penetration, pore formation and endocytosis pathways, have been found for different NP–biomembrane systems.

However, the observation of interactions in real time with a high resolution is still technically challenging because NP–biomembrane interactions occur in microseconds on a temporal scale and nanometers on aspatial scale. In addition, various model lipid bilayer systems are used to study NP–biomembrane interactions. These systems are still too simple to mimic the cell membrane, which limits our comprehensive understanding of NP–biomembrane interactions. Therefore, more complex lipid bilayer membrane models representing real cell membranes are needed. In addition to the limitations of model membranes, the current cell experiments are limited to only particular cell lines, which narrows the understanding of NP–biomembrane interactions, because membrane properties from various cell lines are significantly different. Thus, the systematic investigation of relevant cells is needed in order to understand NP–biomembrane interactions. Finally, the combination of experimental and simulation studies will result in a more convincing understanding of the mechanisms of NP–biomembrane interactions.

Financial & competing interests disclosure

This work was partially supported by the National Natural Science Foundation of China (51322604, 11372243, 21105079 and 81301040), the National 111 Project of China (B06024), the Major International Joint Research Program of China (11120101002), the Key (Key grant) Project of Chinese Ministry of Education (313045), the South Wisdom Valley Innovative Research Team Program, the International Science and Technology Cooperation Program of China (2013DFG02930) and the Fundamental Research Funds for the Central Universities. F Xu was also partially supported by the China Young 1000-Talent Program and the Program for New Century Excellent Talents in University (NCET-12-0437). F Li also acknowledges support from the Science and Technology Research and Development Program by the Shaanxi Province of China (grant. no. 2012K08-18) and the Fundamental Research Funds for the Central Universities (grant no. 2011-0109-08142016 and 2011-010-08143038). BY Sha was also supported by the Program for Youth Science and Technology Star of Shaanxi Province (grant no. 2014KJXX-76). L Wang was supported by the Key Program for International S&T Cooperation Projects of Shaanxi (grant no. 2014KW12-01) and the China Postdoctoral Science Foundation funded project (grant no. 2013M532054). The authors have no other relevant affiliations or financial involvement with any organization or entity with a financial interest in or financial conflict with the subject matter or materials discussed in the manuscript apart from those disclosed.

No writing assistance was utilized in the production of this manuscript.

Executive summary

- Understanding the underlying mechanisms of nanoparticle (NP)–biomembrane interactions is important for enhancing their beneficial effects and avoiding potential nanotoxicities.
- Different NP–biomembrane interactions, including adsorption, penetration, pore formation and endocytosis pathways, have been found for different NP–biomembrane systems.
- Significant achievements regarding the understanding of underlying NP–biomembrane interaction mechanisms have been made by characterizing the morphological, thermal, electromagnetic, optical and electrochemical properties of NP–biomembrane systems and responses of cells and developing mathematical and numerical modeling.
- Real-time monitoring experimental techniques with high resolution and in combination with multiscale simulations are needed in order to improve future studies in this field.

References

Papers of special note have been highlighted as: • of interest

1 Kokura S, Handa O, Takagi T, Ishikawa T, Naito Y, Yoshikawa T. Silver nanoparticles as a safe preservative for use in cosmetics. *Nanomed. Nanotechnol. Biol. Med.* 6(4), 570–574 (2010).

2 Pereira C, Alves C, Monteiro A *et al.* Designing novel hybrid materials by one-pot co-condensation: from hydrophobic mesoporous silica nanoparticles to superamphiphobic cotton textiles. *ACS Appl. Mater. Interfaces* 3(7), 2289–2299 (2011).

3 Cárdenas C, Tobón JI, García C, Vila J. Functionalized building materials: photocatalytic abatement of NOx by cement pastes blended with TiO_2 nanoparticles. *Constr. Build. Mater.* 36, 820–825 (2012).

4 Chen Y, Ding X, Steven Lin S-C *et al.* Tunable nanowire patterning using standing surface acoustic waves. *ACS Nano* 7(4), 3306–3314 (2013).

5 Doane TL, Burda C. The unique role of nanoparticles in nanomedicine: imaging, drug delivery and therapy. *Chem. Soc. Rev.* 41(7), 2885–2911 (2012).

6 Schinwald A, Murphy FA, Jones A, Macnee W, Donaldson K. Graphene-based nanoplatelets: a new risk to the respiratory system as a consequence of their unusual aerodynamic properties. *ACS Nano* 6(1), 736–746 (2011).

7 Baroli B. Penetration of nanoparticles and nanomaterials in the skin: fiction or reality? *J. Pharm. Sci.* 99(1), 21–50 (2010).

8 Lipka J, Semmler-Behnke M, Sperling RA *et al.* Biodistribution of PEG-modified gold nanoparticles following intratracheal instillation and intravenous injection. *Biomaterials* 31(25), 6574–6581 (2010).

9 Peer D, Karp JM, Hong S, Farokhzad OC, Margalit R, Langer R. Nanocarriers as an emerging platform for cancer therapy. *Nat. Nanotechnol.* 2(12), 751–760 (2007).

10 Brannon-Peppas L, Blanchette JO. Nanoparticle and targeted systems for cancer therapy. *Adv. Drug Deliv. Rev.* 56, (11), 1649–1659 (2004).

11 Nam J, Won N, Jin H, Chung H, Kim S. pH-induced aggregation of gold nanoparticles for photothermal cancer therapy. *J. Am. Chem. Soc.* 131(38), 13639–13645 (2009).

12 Dickson KK, Diego AR, Carl AB. Gold hybrid nanoparticles for targeted phototherapy and cancer imaging. *Nanotechnology* 21(10), 105105 (2010).

13 Lewinski N, Colvin V, Drezek R. Cytotoxicity of nanoparticles. *Small* 4(1), 26–49 (2008).

14 Leroueil PR, Berry SA, Duthie K *et al.* Wide varieties of cationic nanoparticles induce defects in supported lipid bilayers. *Nano Lett.* 8(2), 420–424 (2008).

15 Pan Y, Leifert A, Ruau D *et al.* Gold nanoparticles of diameter 1.4 nm trigger necrosis by oxidative stress and mitochondrial damage. *Small* 5(18), 2067–2076 (2009).

16 Wang T, Bai J, Jiang X, Nienhaus GU. Cellular uptake of nanoparticles by membrane penetration: a study combining confocal microscopy with FTIR spectroelectrochemistry. *ACS Nano* 6(2), 1251–1259 (2012).

17 Cho EC, Zhang Q, Xia Y. The effect of sedimentation and diffusion on cellular uptake of gold nanoparticles. *Nat. Nanotechnol.* 6(6), 385–391 (2011).

18 Deloid G, Cohen JM, Darrah T *et al.* Estimating the effective density of engineered nanomaterials for in vitro dosimetry. *Nat. Commun.* 5, 3514 (2014).

19 Yi X, Shi X, Gao H. Cellular uptake of elastic nanoparticles. *Phys. Rev. Lett.* 107(9), 098101 (2011).

20 Shi X, Von Dem Bussche A, Hurt RH, Kane AB, Gao H. Cell entry of one-dimensional nanomaterials occurs by tip recognition and rotation. *Nat. Nanotechnol.* 6(11), 714–719 (2011).

• **Investigates cell entry of 1D nanomaterials using a scanning electron microscopy-based experimental technique and coarse-grained molecular dynamic simulations.**

21 Yang K, Ma Y-Q. Computer simulation of the translocation of nanoparticles with different shapes across a lipid bilayer. *Nat. Nanotechnol.* 5(8), 579–583 (2010).

22 Qu ZG, He XC, Lin M *et al.* Advances in the understanding of nanomaterial–biomembrane interactions and their mathematical and numerical modeling. *Nanomedicine (Lond.)* 8(6), 995–1011 (2013).

• **Illustrates the recent advances in the understanding of nanomaterial–biomembrane interactions based on their numerical modeling.**

23 He X, Qu Z, Xu F *et al.* Molecular analysis of interactions between dendrimers and asymmetric membranes at different transport stages. *Soft Matter* 10(1), 139–148 (2014).

24 Li S, Malmstadt N. Deformation and poration of lipid bilayer membranes by cationic nanoparticles. *Soft Matter* 9(20), 4969–4976 (2013).

25 Goodman CM, Mccusker CD, Yilmaz T, Rotello VM. Toxicity of gold nanoparticles functionalized with cationic and anionic side chains. *Bioconjug. Chem.* 15(4), 897–900 (2004).

26 Vevers W, Jha A. Genotoxic and cytotoxic potential of titanium dioxide (TiO_2) nanoparticles on fish cells *in vitro*. *Ecotoxicology* 17(5), 410–420 (2008).

27 Mecke A, Uppuluri S, Sassanella TM *et al.* Direct observation of lipid bilayer disruption by poly(amidoamine) dendrimers. *Chem. Phys. Lipids* 132(1), 3–14 (2004).

28 Yu J, Patel SA, Dickson RM. *In vitro* and intracellular production of peptide-encapsulated fluorescent silver nanoclusters. *Angew. Chem. Int. Ed. Engl.* 119(12), 2074–2076 (2007).

29 Mu Q, Broughton DL, Yan B. Endosomal leakage and nuclear translocation of multiwalled carbon nanotubes: developing a model for cell uptake. *Nano Lett.* 9(12), 4370–4375 (2009).

30 Foerg C, Merkle HP. On the biomedical promise of cell penetrating peptides: limits versus prospects. *J. Pharm. Sci.* 97(1), 144–162 (2008).

31 Cherukuri P, Bachilo SM, Litovsky SH, Weisman RB. Near-infrared fluorescence microscopy of single-walled carbon nanotubes in phagocytic cells. *J. Am. Chem. Soc.* 126(48), 15638–15639 (2004).

32 Jin H, Heller DA, Strano MS. Single-particle tracking of endocytosis and exocytosis of single-walled carbon nanotubes in NIH-3T3 cells. *Nano Lett.* 8(6), 1577–1585 (2008).

33 Shukla R, Bansal V, Chaudhary M, Basu A, Bhonde RR, Sastry M. Biocompatibility of gold nanoparticles and their endocytotic fate inside the cellular compartment: a microscopic overview. *Langmuir* 21(23), 10644–10654 (2005).

34 Dausend J, Musyanovych A, Dass M *et al.* Uptake mechanism of oppositely charged fluorescent nanoparticles in HeLa cells. *Macromol. Biosci.* 8(12), 1135–1143 (2008).

35 Harush-Frenkel O, Debotton N, Benita S, Altschuler Y. Targeting of nanoparticles to the clathrin-mediated endocytic pathway. *Biochem. Biophys. Res. Commun.* 353(1), 26–32 (2007).

36 Slowing I, Trewyn BG, Lin VSY. Effect of surface functionalization of MCM-41-type mesoporous silica nanoparticles on the endocytosis by human cancer cells. *J. Am. Chem. Soc.* 128(46), 14792–14793 (2006).

37 Rosenholm JM, Meinander A, Peuhu E *et al.* Targeting of porous hybrid silica nanoparticles to cancer cells. *ACS Nano* 3(1), 197–206 (2008).

38 Verma A, Stellacci F. Effect of surface properties on nanoparticle–cell interactions. *Small* 6(1), 12–21 (2010).

39 Cheng LC, Jiang X, Wang J, Chen C, Liu RS. Nano–bio effects: interaction of nanomaterials with cells. *Nanoscale* 5(9), 3547–3569 (2013).

40 Zhao Y, Sun X, Zhang G, Trewyn BG, Slowing II, Lin VSY. Interaction of mesoporous silica nanoparticles with human red blood cell membranes: size and surface effects. *ACS Nano* 5(2), 1366–1375 (2011).

41 Safi M, Courtois J, Seigneuret M, Conjeaud H, Berret JF. The effects of aggregation and protein corona on the cellular internalization of iron oxide nanoparticles. *Biomaterials* 32(35), 9353–9363 (2011).

42 Li Y, Yuan H, Von Dem Bussche A *et al.* Graphene microsheets enter cells through spontaneous membrane penetration at edge asperities and corner sites. *Proc. Natl Acad. Sci. USA* 110(30), 12295–12300 (2013).

43 Gupta A, Curtis AG. Surface modified superparamagnetic nanoparticles for drug delivery: interaction studies with human fibroblasts in culture. *J. Mater. Sci. Mater. Med.* 15(4), 493–496 (2004).

44 Xiao X, Montaño GA, Edwards TL *et al.* Surface charge dependent nanoparticle disruption and deposition of lipid bilayer assemblies. *Langmuir* 28(50), 17396–17403 (2012).

45 Kycia AH, Wang J, Merrill AR, Lipkowski J. Atomic force microscopy studies of a floating-bilayer lipid membrane on a Au(111) surface modified with a hydrophilic monolayer. *Langmuir* 27(17), 10867–10877 (2011).

46 Erickson B, Dimaggio SC, Mullen DG *et al.* Interactions of poly(amidoamine) dendrimers with survanta lung surfactant: the importance of lipid domains. *Langmuir* 24(19), 11003–11008 (2008).

47 Peetla C, Rao KS, Labhasetwar V. Relevance of biophysical interactions of nanoparticles with a model membrane in predicting cellular uptake: study with TAT peptide-conjugated nanoparticles. *Mol. Pharm.* 6(5), 1311–1320 (2009).

48 Roiter Y, Ornatska M, Rammohan AR, Balakrishnan J, Heine DR, Minko S. Interaction of nanoparticles with lipid membrane. *Nano Lett.* 8(3), 941–944 (2008).

49 Hong S, Bielinska AU, Mecke A *et al.* Interaction of poly(amidoamine) dendrimers with supported lipid bilayers and cells: hole formation and the relation to transport. *Bioconjug. Chem.* 15(4), 774–782 (2004).

50 Hong S, Leroueil PR, Janus EK *et al.* Interaction of polycationic polymers with supported lipid bilayers and cells: nanoscale hole formation and enhanced membrane permeability. *Bioconjug. Chem.* 17(3), 728–734 (2006).

51 Mecke A, Lee D-K, Ramamoorthy A, Orr BG, Banaszak Holl MM. Synthetic and natural polycationic polymer nanoparticles interact selectively with fluid-phase domains of DMPC lipid bilayers. *Langmuir* 21(19), 8588–8590 (2005).

52 Roiter Y, Ornatska M, Rammohan AR, Balakrishnan J, Heine DR, Minko S. Interaction of lipid membrane with nanostructured surfaces. *Langmuir* 25(11), 6287–6299 (2009).

53 Morandat S, Azouzi S, Beauvais E, Mastouri A, El Kirat K. Atomic force microscopy of model lipid membranes. *Anal. Bioanal. Chem.* 405(5), 1445–1461 (2013).

54 Cho S-J, Cho N-J, Anh JH, Jung G-E, Anariba F. Biophysical applications of scanning ion conductance microscopy (SICM). *Mod. Phys. Lett. B* 26(05), 1130003 (2012).

55 Chen C-C, Zhou Y, Baker LA. Scanning ion conductance microscopy. *Annu. Rev. Anal. Chem.* 5(1), 207–228 (2012).

56 Ruenraroengsak P, Novak P, Berhanu D *et al.* Respiratory epithelial cytotoxicity and membrane damage (holes) caused by amine-modified nanoparticles. *Nanotoxicology* 6(1), 94–108 (2012).

57 Yang X, Liu X, Lu H *et al.* Real-time investigation of acute toxicity of ZnO nanoparticles on human lung epithelia with hopping probe ion conductance microscopy. *Chem. Res. Toxicol.* 25(2), 297–304 (2011).

58 Gorelik J, Shevchuk A, Ramalho M *et al.* Scanning surface confocal microscopy for simultaneous topographical and fluorescence imaging: application to single virus-like particle entry into a cell. *Proc. Natl Acad. Sci. USA* 99(25), 16018–16023 (2002).

59 Miragoli M, Novak P, Ruenraroengsak P *et al.* Functional interaction between charged nanoparticles and cardiac tissue: a new paradigm for cardiac arrhythmia? *Nanomedicine* 8(5), 725–737 (2012).

60 Montenegro L, Ottimo S, Puglisi G, Castelli F, Sarpietro MG. Idebenone loaded solid lipid nanoparticles interact with biomembrane models: calorimetric evidence. *Mol. Pharm.* 9(9), 2534–2541 (2012).

• **Investigates the interaction of idebenone-loaded solid lipid nanoparticles with multilamellar vesicles using the differential scanning calorimetry method.**

61 Wrobel D, Ionov M, Gardikis K *et al.* Interactions of phosphorus-containing dendrimers with liposomes. *Biochim. Biophys. Acta* 1811(3), 221–226 (2011).

62 Gupta A, Mandal D, Ahmadibeni Y, Parang K, Bothun G. Hydrophobicity drives the cellular uptake of short cationic peptide ligands. *Eur. Biophys. J.* 40(6), 727–736 (2011).

63 Alves ID, Goasdoue N, Correia I *et al.* Membrane interaction and perturbation mechanisms induced by two cationic cell penetrating peptides with distinct charge distribution. *Biochim. Biophys. Acta* 1780(7–8), 948–959 (2008).

64 Walde P, Cosentino K, Engel H, Stano P. Giant vesicles: preparations and applications. *ChemBioChem* 11(7), 848–865 (2010).

65 Warschawski DE, Arnold AA, Beaugrand M, Gravel A, Chartrand , Marcotte I. Choosing membrane mimetics for NMR structural studies of transmembrane proteins. *Biochim. Biophys. Acta* 1808(8), 1957–1974 (2011).

66 Brisebois P, Arnold A, Chabre Y, Roy R, Marcotte I. Comparative study of the interaction of fullerenol nanoparticles with eukaryotic and bacterial model membranes using solid-state NMR and FTIR spectroscopy. *Eur. Biophys. J.* 41(6), 535–544 (2012).

67 Wrobel D, Kłys A, Ionov M *et al.* Cationic carbosilane dendrimers–lipid membrane interactions. *Chem. Phys. Lipids* 165(4), 401–407 (2012).

68 Smith PES, Brender JR, Dürr UHN *et al.* Solid-state NMR reveals the hydrophobic-core location of poly(amidoamine) dendrimers in biomembranes. *J. Am. Chem. Soc.* 132(23), 8087–8097 (2010).

69 Choi D, Moon JH, Kim H *et al.* Insertion mechanism of cell-penetrating peptides into supported phospholipid membranes revealed by x-ray and neutron reflection. *Soft Matter* 8(32), 8294–8297 (2012).

70 Vandoolaeghe P, Rennie AR, Campbell RA, Nylander T. Neutron reflectivity studies of the interaction of cubic-phase nanoparticles with phospholipid bilayers of different coverage†. *Langmuir* 25(7), 4009–4020 (2008).

71 Vandoolaeghe P, Rennie AR, Campbell RA *et al.* Adsorption of cubic liquid crystalline nanoparticles on model membranes. *Soft Matter* 4(11), 2267–2277 (2008).

72 Tantra R, Knight A. Cellular uptake and intracellular fate of engineered nanoparticles: a review on the application of imaging techniques. *Nanotoxicology* 5(3), 381–392 (2011).

73 Al-Jamal WT, Al-Jamal KT, Tian B *et al.* Lipid–quantum dot bilayer vesicles enhance tumor cell uptake and retention *in vitro* and *in vivo*. *ACS Nano* 2(3), 408–418 (2008).

74 Fazlollahi F, Sipos A, Kim YH *et al.* Translocation of PEGylated quantum dots across rat alveolar epithelial cell monolayers. *Int. J. Nanomedicine* 6, 2849–2857 (2011).

75 Ghosh P, Yang X, Arvizo R *et al.* Intracellular delivery of a membrane-impermeable enzyme in active form using functionalized gold nanoparticles. *J. Am. Chem. Soc.* 132(8), 2642–2645 (2010).

76 Kelf TA, Sreenivasan VKA, Sun J, Kim EJ, Goldys EM, Zvyagin AV. Non-specific cellular uptake of surface-functionalized quantum dots. *Nanotechnology* 21(28), 285105 (2010).

77 Xu AM, Aalipour A, Leal-Ortiz S *et al.* Quantification of nanowire penetration into living cells. *Nat. Commun.* 5, 3613 (2014).

78 Jin H, Heller DA, Sharma R, Strano MS. Size-dependent cellular uptake and expulsion of single-walled carbon nanotubes: single particle tracking and a generic uptake model for nanoparticles. *ACS Nano* 3(1), 149–158 (2009).

79 Ciobanasu C, Harms E, TüNnemann G, Cardoso MC, Kubitscheck U. Cell-penetrating HIV1 TAT peptides float on model lipid bilayers. *Biochemistry* 48(22), 4728–4737 (2009).

80 Ciobanasu C, Siebrasse JP, Kubitscheck U. Cell-penetrating HIV1 TAT peptides can generate pores in model membranes. *Biophys. J.* 99(1), 153–162 (2010).

81 Mascalchi P, Haanappel E, Carayon K, Mazeres S, Salome L. Probing the influence of the particle in single particle tracking measurements of lipid diffusion. *Soft Matter* 8(16), 4462–4470 (2012).

82 Welsher K, Yang H. Multi-resolution 3D visualization of the early stages of cellular uptake of peptide-coated nanoparticles. *Nat. Nanotechnol.* 9(3), 198–203 (2014).

• **Presents a newly developed technology that is able to capture the landing process of nanoparticles in real time before cellular uptake in 3D manner.**

83 Han Y, Wang X, Dai H, Li S. Nanosize and surface charge effects of hydroxyapatite nanoparticles on red blood cell suspensions. *ACS Appl. Mater. Interfaces* 4(9), 4616–4622 (2012).

84 Levin CS, Kundu J, Janesko BG, Scuseria GE, Raphael RM, Halas NJ. Interactions of ibuprofen with hybrid lipid bilayers probed by complementary surface-enhanced vibrational spectroscopies. *J. Phys. Chem. B* 112(45), 14168–14175 (2008).

85 Bard AJ, Li X, Zhan W. Chemically imaging living cells by scanning electrochemical microscopy. *Biosens. Bioelectron.* 22(4), 461–472 (2006).

86 Chen Z, Xie S, Shen L *et al.* Investigation of the interactions between silver nanoparticles and HeLa cells by scanning electrochemical microscopy. *Analyst* 133(9), 1221–1228 (2008).

87 Zhan D, Li X, Nepomnyashchii AB, Alpuche-Aviles MA, Fan F-RF, Bard AJ. Characterization of Ag^+ toxicity on living fibroblast cells by the ferrocenemethanol and oxygen response with the scanning electrochemical microscope. *J. Electroanal. Chem.* 688, 61–68 (2013).

88 Prasanth R, Gopinath D. Effect of ZnO nanoparticles on nasopharyngeal cancer cells viability and respiration. *Appl. Phys. Lett.* 102(11), 113702 (2013).

89 Verma A, Uzun O, Hu Y *et al.* Surface-structure-regulated cell-membrane penetration by monolayer-protected nanoparticles. *Nat. Mater.* 7(7), 588–595 (2008).

90 Cebrián V, Martín-Saavedra F, Yagüe C, Arruebo M, Santamaría J, Vilaboa N. Size-dependent transfection efficiency of PEI-coated gold nanoparticles. *Acta Biomater.* 7(10), 3645–3655 (2011).

91 Zhu Y, Li W, Li Q *et al.* Effects of serum proteins on intracellular uptake and cytotoxicity of carbon nanoparticles. *Carbon* 47(5), 1351–1358 (2009).

92 Luo R, Neu B, Venkatraman SS. Surface functionalization of nanoparticles to control cell interactions and drug release. *Small* 8(16), 2585–2594 (2012).

93 Champion JA, Mitragotri S. Role of target geometry in phagocytosis. *Proc. Natl Acad. Sci. USA* 103(13), 4930–4934 (2006).

94 Gonzalez L, Lison D, Kirsch-Volders M. Genotoxicity of engineered nanomaterials: a critical review. *Nanotoxicology* 2(4), 252–273 (2008).

95 Xia T, Korge P, Weiss JN *et al.* Quinones and aromatic chemical compounds in particulate matter induce mitochondrial dysfunction: implications for ultrafine particle toxicity. *Environ. Health Perspect.* 112(14), 1347–1358 (2004).

96 Foster KA, Galeffi F, Gerich FJ, Turner DA, Muller M. Optical and pharmacological tools to investigate the role of mitochondria during oxidative stress and neurodegeneration. *Prog. Neurobiol.* 79(3), 136–171 (2006).

97 Buettner GR. The pecking order of free radicals and antioxidants: lipid peroxidation, α-tocopherol, and ascorbate. *Arch. Biochem. Biophys.* 300(2), 535–543 (1993).

98 Pryor WA, Stanley JP. A suggested mechanism for the production of malonaldehyde during the autoxidation of polyunsaturated fatty acids. Nonenzymatic production of prostaglandin endoperoxides during autoxidation. *J. Org. Chem.* 40(24), 3615–3617 (1975).

99 Mahreen R, Mohsin M, Nasreen Z, Siraj M, Ishaq M. Significantly increased levels of serum malonaldehyde in Type 2 diabetics with myocardial infarction. *Int. J. Diabetes Dev. Ctries* 30(1), 49–51 (2010).

100 Zhao X, Wang S, Wu Y, You H, Lv L. Acute ZnO nanoparticles exposure induces developmental toxicity, oxidative stress and DNA damage in embryo–larval zebrafish. *Aquat. Toxicol.* 136–137, 49–59 (2013).

101 Xu J, Li Z, Xu P, Xiao L, Yang Z. Nanosized copper oxide induces apoptosis through oxidative stress in podocytes. *Arch. Toxicol.* 87(6), 1067–1073 (2013).

102 Li JJ, Hartono D, Ong C-N, Bay B-H, Yung L-YL. Autophagy and oxidative stress associated with gold nanoparticles. *Biomaterials* 31(23), 5996–6003 (2010).

103 Corsi K, Chellat F, Yahia L, Fernandes JC. Mesenchymal stem cells, MG63 and HEK293 transfection using chitosan–DNA nanoparticles. *Biomaterials* 24(7), 1255–1264 (2003).

104 Vevers WF, Jha AN. Genotoxic and cytotoxic potential of titanium dioxide (TiO_2) nanoparticles on fish cells *in vitro*. *Ecotoxicology* 17(5), 410–420 (2008).

105 Haslam G, Wyatt D, Kitos PA. Estimating the number of viable animal cells in multi-well cultures based on their lactate dehydrogenase activities. *Cytotechnology* 32(1), 63–75 (2000).

106 Yao KA, Huang DQ, Xu BL, Wang N, Wang YJ, Bi SP. A sensitive electrochemical approach for monitoring the effects of nano-Al_2O_3 on LDH activity by differential pulse voltammetry. *Analyst* 135(1), 116–120 (2010).

107 Yu KO, Grabinski CM, Schrand AM *et al.* Toxicity of amorphous silica nanoparticles in mouse keratinocytes. *J. Nanopart. Res.* 11(1), 15–24 (2009).

108 Song M-M, Song W-J, Bi H *et al.* Cytotoxicity and cellular uptake of iron nanowires. *Biomaterials* 31(7), 1509–1517 (2010).

109 Akagi T, Kim H, Akashi M. pH-dependent disruption of erythrocyte membrane by amphiphilic poly(amino acid) nanoparticles. *J. Biomater. Sci. Polym. Ed.* 21(3), 315–328 (2010).

110 Kim K-J, Sung W, Suh B *et al.* Antifungal activity and mode of action of silver nano-particles on Candida albicans. *Biometals* 22(2), 235–242 (2009).

111 Nawaz S, Redhead M, Mantovani G, Alexander C, Bosquillon C, Carbone P. Interactions of PEO–PPO–PEO block copolymers with lipid membranes: a computational and experimental study linking membrane lysis with polymer structure. *Soft Matter* 8(25), 6744–6754 (2012).

112 Monticelli L, Salonen E. *Biomolecular Simulations – Methods and Protocols*. Springer, Germany (2013).

113 Porasso RD, Bennett WF, Oliveira-Costa SD, Lopez Cascales JJ. Study of the benzocaine transfer from aqueous solution to the interior of a biological membrane. *J. Phys. Chem. B* 113(29), 9988–9994 (2009).

114 Chang R-W, Lee J-M. Dynamics of C60 molecules in biological membranes. Computer simulation studies. *Bull. Korean Chem. Soc.* 31(11), 3195–3200 (2010).

115 Li L, Davande H, Bedrov D, Smith GD. A molecular dynamics simulation study of C60 fullerenes inside a dimyristoylphosphatidylcholine lipid bilayer. *J. Phys. Chem. B* 111(16), 4067–4072 (2007).

116 Ingólfsson HI, Lopez CA, Uusitalo JJ *et al.* The power of coarse graining in biomolecular simulations. *Wiley Interdiscip. Rev. Comput. Mol. Sci.* 4(3), 225–248 (2013).

117 Wong-Ekkabut J, Baoukina S, Triampo W, Tang IM, Tieleman DP, Monticelli L. Computer simulation study of fullerene translocation through lipid membranes. *Nat. Nanotechnol.* 3(6), 363–368 (2008).

118 Lunov O, Zablotskii V, Syrovets T *et al.* Modeling receptor-mediated endocytosis of polymer-functionalized iron oxide nanoparticles by human macrophages. *Biomaterials* 32(2), 547–555 (2011).

119 Gao H, Shi W, Freund LB. Mechanics of receptor-mediated endocytosis. *Proc. Natl. Acad. Sci. USA* 102(27), 9469–9474 (2005).

120 Yi X, Shi X, Gao H. A universal law for cell uptake of one-dimensional nanomaterials. *Nano Lett.* 14(2), 1049–1055 (2014).

121 Andreasson-Ochsner M, Romano G, Hakanson M *et al.* Single cell 3-D platform to study ligand mobility in cell–cell contact. *Lab Chip* 11(17), 2876–2883 (2011).

122 Frost R, Jönsson GE, Chakarov D, Svedhem S, Kasemo B. Graphene oxide and lipid membranes: interactions and nanocomposite structures. *Nano Lett.* 12(7), 3356–3362 (2012).

123 Frost R, Grandfils C, Cerda B, Kasemo B, Svedhem S. Structural rearrangements of polymeric insulin-loaded nanoparticles interacting with surface-supported model lipid membranes. *J. Biomater. Nanobiotechnol.* 2 (2), 181–193 (2011).

124 Akesson A, Lundgaard CV, Ehrlich N, Pomorski TG, Stamou D, Cardenas M. Induced dye leakage by PAMAM

G6 does not imply dendrimer entry into vesicle lumen. *Soft Matter* 8(34), 8972–8980 (2012).

125 Ojea-Jiménez I, García-Fernández L, Lorenzo J, Puntes VF. Facile preparation of cationic gold nanoparticle-bioconjugates for cell penetration and nuclear targeting. *ACS Nano* 6(9), 7692–7702 (2012).

126 Hou W-C, Moghadam BY, Corredor C, Westerhoff P, Posner JD. Distribution of functionalized gold nanoparticles between water and lipid bilayers as model cell membranes. *Environ. Sci. Technol.* 46(3), 1869–1876 (2012).

127 Hou W-C, Moghadam BY, Westerhoff P, Posner JD. Distribution of fullerene nanomaterials between water and model biological membranes. *Langmuir* 27(19), 11899–11905 (2011).

128 Carney RP, Astier Y, Carney TM, Voïtchovsky K, Jacob Silva PH, Stellacci F. Electrical method to quantify nanoparticle interaction with lipid bilayers. *ACS Nano* 7(2), 932–942 (2012).

129 Zupanc J, Drobne D, Drasler B *et al.* Experimental evidence for the interaction of C-60 fullerene with lipid vesicle membranes. *Carbon* 50(3), 1170–1178 (2012).

130 Parimi S, Barnes TJ, Callen DF, Prestidge CA. Mechanistic insight into cell growth, internalization, and cytotoxicity of PAMAM dendrimers. *Biomacromolecules* 11(2), 382–389 (2009).

131 Zhang S, Nelson A, Beales PA. Freezing or wrapping: the role of particle size in the mechanism of nanoparticle–biomembrane interaction. *Langmuir* 28(35), 12831–12837 (2012).

132 Cho EC, Liu Y, Xia Y. A simple spectroscopic method for differentiating cellular uptakes of gold nanospheres and nanorods from their mixtures. *Angew. Chem. Int. Ed.* 49(11), 1976–1980 (2010).

133 Ke PC, Lamm MH. A biophysical perspective of understanding nanoparticles at large. *Phys. Chem. Chem. Phys.* 13(16), 7273–7283 (2011).

134 Barauskas J, Cervin C, Jankunec M *et al.* Interactions of lipid-based liquid crystalline nanoparticles with model and cell membranes. *Int. J. Pharm.* 391(1–2), 284–291 (2010).

135 kesson A, Lind TK, Barker R, Hughes A, Cárdenas M. Unraveling dendrimer translocation across cell membrane mimics. *Langmuir* 28(36), 13025–13033 (2012).